Applied Catalysis B: Environmental 87 (2009) 56–62

Contents lists available at ScienceDirect

Applied Catalysis B: Environmental

journal homepage: www.elsevier.com/locate/apcatb

Investigation of the photocatalytic degradation of brown water natural organic matter by size exclusion chromatography

Luis A. Tercero Espinoza *, Eike ter Haseborg, Matthias Weber, Fritz H. Frimmel

Water Chemistry, Engler-Bunte-Institut, Universität Karlsruhe (TH), Engler-Bunte-Ring 1, 76131 Karlsruhe, Germany

ARTICLE INFO

Article history:
Received 27 June 2008
Received in revised form 1 August 2008
Accepted 17 August 2008
Available online 22 August 2008

Keywords:
Heterogeneous photocatalysis
Titanium dioxide
Natural organic matter
Size exclusion chromatography
Bioavailability

ABSTRACT

Herein we report on the photocatalytic degradation of natural organic matter from a bog lake (Lake Hohloh, Black Forest, Germany) as followed by size exclusion chromatography with dissolved organic carbon (DOC) and ultraviolet ($\lambda = 254$ nm) detection (SEC-DOC and SEC-UV). When irradiating this humic-rich water in the presence of 0.5 g L^{-1} titanium dioxide (P25), we found a preferential degradation of the higher molecular weight DOC fraction. This was coupled to growth of the middle and small DOC fractions. Mineralization proceeded in two distinct steps: a first stage without noticeable mineralization, followed by a phase of steady decrease in dissolved organic carbon. Formic, oxalic, succinic and glutaric acids were found in the irradiated samples and contribute significantly to the bioavailable DOC after irradiation, which favors bacterial regrowth.

1. Introduction

Natural organic matter (NOM) is ubiquitous in natural waters and plays a fundamental role in the aquatic environment. However, in water for human consumption, NOM is also the main natural precursor of unwanted haloorganic disinfection byproducts (DBPs), of which trihalomethanes (THMs) are the most prominent example [1,2]. As such, it is critical to understand the behavior of NOM in established and possibly alternative water treatment steps.

We report on the degradation of NOM in heterogeneous photocatalysis with suspended titanium dioxide (TiO_2) nanoparticle agglomerates as the photocatalyst. The effectiveness of this process is based largely on the action of hydroxyl radicals (•OH), a short-lived and extremely potent oxidizing agent, which are formed from adsorbed OH^- and H_2O on the surface of TiO_2 following band-gap illumination ($\lambda < 388$ nm) [3,4]. As a water treatment process, heterogeneous photocatalysis has been shown to be effective for the removal of a wide variety of organic micropollutants and continues to attract the attention of researchers around the globe, especially from countries with an ample supply of sunshine, which can be used to provide the otherwise expensive photons required (e.g. [5]). As such, this process has deployment potential in small, decentralized water treatment units using solar radiation as an energy source.

The study of the photocatalytic degradation of NOM, especially humic acids, in TiO_2 photocatalysis has been focused on the reduction of the THM formation potential [6], on the reduction of color [7–9], and on the different factors influencing the velocity of reaction [10–14]. The techniques used to study this process include ultraviolet–visible (UV–vis), infrared (IR) and fluorescence spectroscopies, as well as total organic carbon (TOC) measurements. However, less effort has gone into showing the evolution of molecular size in a natural water rich in humic material. Noteworthy among these are the studies of Uyguner and Bekbölet [9] and Kerc et al. [15] who used ultrafiltration to fractionate humic material before and after irradiation in TiO_2 suspensions, and the study by Wiszniowski et al. [16], who used a high performance liquid chromatography (HPLC) setup equipped with a carbohydrate column to fractionate model humic material before and after irradiation.

With the work presented herein, we aimed to contribute to the understanding of the photocatalytic degradation of NOM by quantifying the changes in molecular size and UV absorption ($\lambda = 254$ nm), as measured by size exclusion chromatography (SEC), which occur during the course of the UV irradiation in the presence of a TiO_2 photocatalyst. These changes are important because they can lead to different reactivity of NOM, especially towards chlorine, thus affecting the THM formation potential [17]. Furthermore, changes in the molecular structure and size distribution of NOM can lead to increased bioavailability of the dissolved organic carbon (DOC), favoring bacterial regrowth [18]. In order to characterize this,

* Corresponding author. Fax: +49 721 608 7051.
E-mail addresses: luis.tercero@ebi-wasser.uni-karlsruhe.de (L.A. Tercero Espinoza), fritz.frimmel@ebi-wasser.uni-karlsruhe.de (F.H. Frimmel).

0926-3373/$ – see front matter © 2008 Elsevier B.V. All rights reserved.
doi:10.1016/j.apcatb.2008.08.013

we examined the production of small organic acids and the bioavailability of the organic material after irradiation.

As a source of NOM, we turned to humic-rich brown water from a bog lake (Lake Hohloh, Black Forest, Germany). This brown water has been extensively used as a reference material to study the characteristics and behavior of aquatic NOM (e.g. [1], and references therein).

2. Materials and methods

2.1. Irradiation procedure

Twenty milligrams of TiO_2 (P25, Degussa, Germany) were suspended in 40 mL of lake Hohloh water, previously filtered through 0.45 μm cellulose acetate membrane filters. The concentration of dissolved organic carbon in the filtered Lake Hohloh water was $\rho(\mathrm{DOC}) = 21\ \mathrm{mg\ L^{-1}}$. Lake Hohloh water is extensively described elsewhere [1]. Samples were sonicated for 10 min prior to irradiation.

The samples were irradiated using a solar UV simulator (Oriel Corp., Stratford, CT, USA) with an atmospheric attenuation filter (Oriel Corp., Stratford, CT) installed in the radiation beam. The scheme of the solar simulator used for irradiation experiments is described elsewhere [19]. The samples were stirred, open to the atmosphere, and irradiated from above by a homogeneous light field. The sample volume was 40 mL in all experiments, with an irradiation pathlength of ≈ 3.5 cm.

The incident photon flux was determined by chemical polychromatic actinometry using phenylglyoxylic acid in a mixture of acetonitrile (AcN) and Milli-Q water (AcN:Milli-Q water = 3:1, v/v) [20]. The photon flow in the UV range ($290 < \lambda < 400$ nm) of the solar UV simulator estimated by this method was 1×10^{-7} einstein $\mathrm{s^{-1}}$.

2.2. Size exclusion chromatography with dissolved organic carbon and ultraviolet detection (SEC-DOC and SEC-UV)

Size exclusion chromatograms were recorded using the SEC-DOC/UV system described by Huber and Frimmel [21]. In this system, a photochemical oxidation of the sample components is carried out using a low-pressure mercury lamp in a rotating thin-film reactor. Toyopearl HW 50S resin (Tosoh Corp., Japan) packed in a Novogrom column (length: 250 mm, inner diameter: 20 mm; Alltech Grom, Germany) served as stationary phase, while phosphate eluent ($1.5\ \mathrm{g\ L^{-1}} Na_2HPO_4 \cdot 2H_2O + 2.5\ \mathrm{g\ L^{-1}}\ KH_2PO_4$) flowing at a rate of 1 mL $\mathrm{min^{-1}}$ served as the mobile phase for separation. Samples were filtered (0.45 μm) and diluted 1:5 prior to analysis. The injection volume was 1 mL and the DOC concentration of each sample was calculated on the basis of an external calibration using potassium hydrogen phthalate as a standard.

Under these conditions, totally excluded molecules eluted after a retention time, $t_r = 28.7$ min (t_e), while totally permeating molecules eluted after $t_r = 66.3$ min (t_p). The dimensionless distribution coefficient, K_D is often used for comparison purposes and is defined as

$$K_D = \frac{t_r - t_e}{t_p - t_e} \quad (1)$$

Thus, molecules whose t_r is determined primarily through size exclusion elute with $0 < K_D < 1$. Hydrophobic interactions of the analyte molecules with the column packing material lead to longer t_r, and strongly interacting analytes may remain attached to the column material [22].

Ultraviolet absorption was recorded at $\lambda = 254$ nm.

2.3. Ion chromatography (IC)

The determination of low molecular weight organic acids on filtered samples (0.45 μm) was performed with ion exchange chromatography with conductivity detection after suppression using a Dionex DX500 system, equipped with an IonPac® AS11 column (length 250 mm, diameter 4 mm) with AG11 pre-column (length 50 mm, diameter 4 mm), and an ASRS Ultra suppressor coupled to an ED40 conductivity detector. The eluent was aqueous KOH with concentrations: $c(\mathrm{OH^-}) = 35\ \mathrm{mmol\ L^{-1}}$ over 10 min for regeneration of the column, $c(\mathrm{OH^-}) = 0.20\ \mathrm{mmol\ L^{-1}}$ for 5 min (equilibration) followed by a linear increase to $c(\mathrm{OH^-}) = 15.0\ \mathrm{mmol\ L^{-1}}$ over 10 min immediately after injection of the sample, followed by a further linear increase to $c(\mathrm{OH^-}) = 21.7\ \mathrm{mmol\ L^{-1}}$ over 5 min. The gradient was prepared using Milli-Q® water previously degassed with helium (5.0).

2.4. Degradation experiments with bacteria from activated sludge

The biodegradability of the irradiated samples was estimated by performing SEC-DOC measurements of filtered samples after incubation with a mixed bacterial culture. Briefly, 4 mL of activated sludge inoculum (mixed from two wastewater treatment plants, one municipal and one industrial) were added to 50 mL of the irradiated samples (filtered 0.45 μm to remove the TiO_2 particles). The samples were then incubated on a shaker (70 rpm) kept in the dark for 48 h at 36 °C.

3. Results and discussion

3.1. Size exclusion chromatography with dissolved organic carbon detection (SEC-DOC)

The SEC-DOC chromatograms of the samples before and after simulated solar UV irradiation were divided into three fractions for ease of analysis, as shown on the left panel of Fig. 1. The fractions are also referred to as F1–F3 in the following presentation and discussion. All irradiation experiments were performed in the presence of $\rho(TiO_2) = 0.5\ \mathrm{g\ L^{-1}}$, where ρ denotes a mass concentration.

F1 was defined to lie in the interval $28.0\ \mathrm{min} < t_r < 45.8$ min, where t_r is the retention time (in this study numerically equal to the elution volume in mL). It appears to be composed of two overlapping peaks, the higher one with maximum at $t_r = 41.9$ min and the shorter one (shoulder) with maximum around $t_r = 43.5$ min. These two peaks are commonly attributed to humic material [23]. F2 ($45.8\ \mathrm{min} < t_r < 50.7$ min, maximum of the underlying peak around $t_r = 46.8$ min) constitutes a second shoulder in the chromatogram of the non-irradiated lake Hohloh water samples. This fraction becomes important upon irradiation and thus deserves separate consideration (see Fig. 1). The DOC contained in F2 is sometimes referred to as "building blocks" and is assumed to contain aromatic and polyfunctional organic acids [23,24]. The third fraction, F3 ($50.7\ \mathrm{min} < t_r < 56.5$ min), appears clearly as a peak with maximum at $t_r = 52.7$ min in the chromatograms of both non-irradiated and irradiated lake Hohloh samples. Because the samples were not buffered prior to injection into the SEC-DOC system, this last peak also includes molecules that elute prematurely due to the difference in ionic strength between sample and mobile phase [23,22].

Upon irradiation, we observed a rapid reduction in F1, accompanied by an increase in both F2 and F3. Assuming size exclusion to be the dominant fractionation mechanism [18], the decrease in DOC content of F1 comes from the loss of the larger portion of F1 (shorter t_r). While the maximum in F1 shifted from

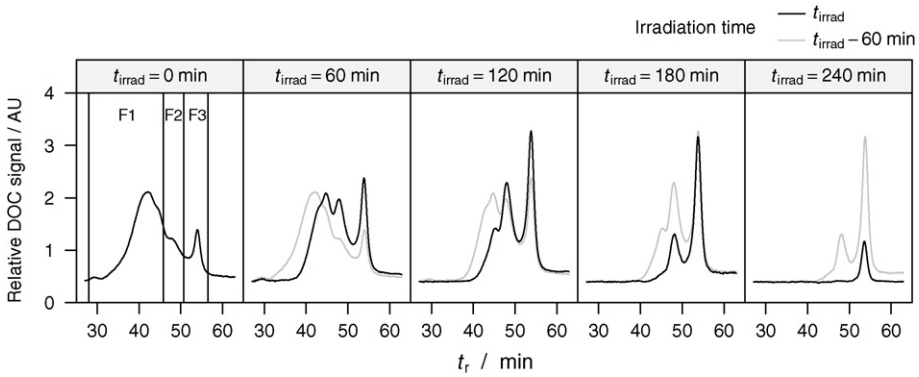

Fig. 1. SEC-DOC chromatograms showing the defined fractions (F1–F3) and their time evolution under UV irradiation in the presence of $\rho(TiO_2) = 0.5\ g\ L^{-1}$.

the larger to the smaller of the two overlapping peaks, the maxima of the peaks in F2 and F3 eluted at the same time throughout the course of irradiation. Altogether, Fig. 1 shows a continuous shift of the SEC-DOC chromatograms towards longer retention times (t_r) with increasing irradiation time (t_{irrad}). This is evidence for a steady decrease in mean molecular size of the NOM during the course of irradiation.

The decrease in DOC content of F1 was linear for $t_{irrad} \leq 120$ min, with a rate of decrease in DOC $\approx 0.05\ mg\ L^{-1}\ min^{-1}$ (Fig. 2). F2 and F3 increased linearly during the first hour of irradiation, each at a rate approximately half that of decrease of F1, resulting in a nearly constant sum of the DOC content in the defined fractions. F2 reached a maximum after ≈90 min of irradiation and decreased afterwards. F3 increased up to $t_{irrad} \approx 150$ min and also decreased afterwards. The steady decrease in F1, together with the decrease in F2 and slower increase in F3 led to an overall decrease of the DOC contained in F1–F3 starting in the second hour of irradiation.

The degradation of NOM should proceed largely unselectively due to the dominant role of OH-radicals in heterogeneous photocatalysis [4,25]. Rate constants for the reaction of •OH with NOM are typically on the order of $10^8\ M^{-1}\ s^{-1}$[25]. However, inspection of Fig. 1 clearly shows the growth of the smaller fractions F2 and F3 at the cost of F1. The reason for this is that degradation of F1 does not immediately lead to mineralization but

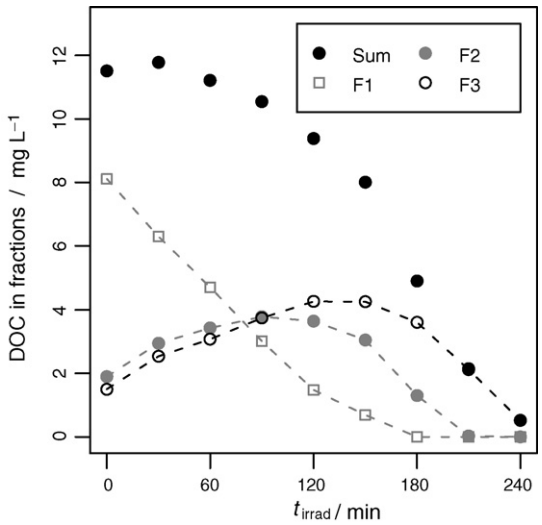

Fig. 2. DOC content of each fraction as a function of irradiation time in the presence of $\rho(TiO_2) = 0.5\ g\ L^{-1}$. The dashed lines are intended as a guide to the eye. The filled black dots correspond to the sum of the DOC contained in F1, F2 and F3 and therefore do not represent all DOC accessible to analysis by size exclusion chromatography (cDOC).

to the formation of smaller metabolites, largely contained in F2 and F3. The DOC content of F1–F3 is thus determined by its initial DOC content plus the surplus or deficit arising from differences in its rates of formation and degradation. Since there are no fractions larger than F1, it can only be degraded into smaller molecules, thus decreasing steadily throughout the course of irradiation. F2 initially grows as F1 is degraded but reaches a maximum and declines as F1 becomes smaller. F3 shows similar behavior.

The dynamics of the process resemble the degradation of a single parent compound over two intermediates. Inspection of Fig. 2 reveals three stages of degradation as follows:

(1) $0\ min < t_{irrad} \leq 60$ min—in this initial stage the degradation of F1 dominated, leading to increasing F2 and F3 such that the sum of the DOC contained in all fractions remained nearly constant.
(2) $60\ min \leq t_{irrad} \leq 150$ min—after approximately 1 h of irradiation, the degradation of F2/F3 started to become important, leading to mineralization. The DOC content of F2 did not change considerably ($3.4 \pm 0.3\ mg\ L^{-1}$), indicating nearly equal rates of formation and degradation for this fraction. The DOC content of F3 continues to grow during this stage and the rate of degradation of F1 becomes smaller towards the end, when it is nearly depleted.
(3) $150\ min < t_{irrad} \leq 240$ min—because of the nearly complete disappearance of F1 after $t_{irrad} = 150$ min, the DOC content of F2 decreases more rapidly after this point (essentially no more formation of F2 from F1). At the same time, F3 reaches its maximum and decreases steadily for $t_{irrad} > 150$ min. This leads to a faster mineralization rate compared to that of the second stage. At the end of the irradiation, all remaining DOC is contained in F3 and being rapidly degraded.

Since the photocatalyst was removed by membrane filtration before analysis, the results obtained in this study are valid only for the aqueous phase of the titanium dioxide suspensions. Moreover, we note that there is a considerable amount of DOC which adsorbs onto the surface of the photocatalyst and is not accessible to fractionation by SEC (cf. [8,26,27]). In our case, approximately 37% of the DOC accessible for SEC-DOC analysis adsorbed to the photocatalyst prior to illumination. This is seen in Fig. 3, which shows SEC-DOC chromatograms of Lake Hohloh water prior to and after 15 and 60 min of contact with $0.5\ g\ L^{-1}\ TiO_2$ in the dark. No significant changes in the chromatograms could be observed after 1 h of adsorption time in the dark.

Inspection of the chromatograms shown in Fig. 3 reveals that F1 adsorbs to a larger extent onto the surface of TiO_2 than both F2 and F3 ($\approx 6.1\ mg\ L^{-1}$ vs. $\approx 0.4\ mg\ L^{-1}$ and $\approx 0.3\ mg\ L^{-1}$ respectively

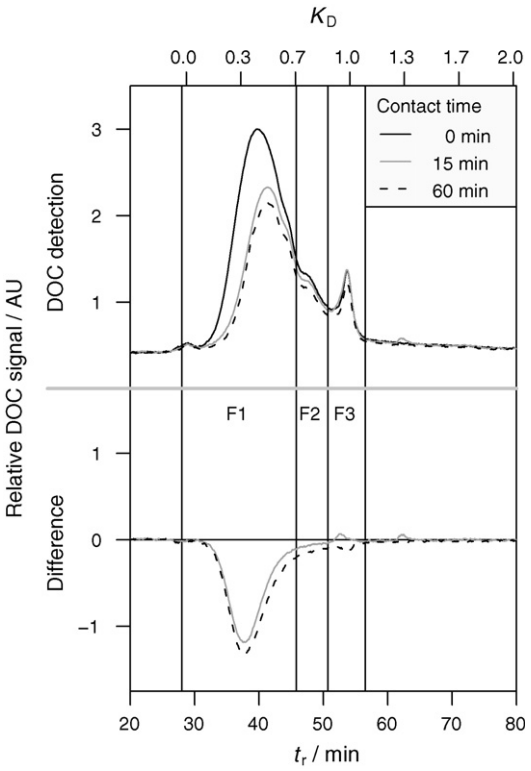

Fig. 3. SEC-DOC chromatograms showing the adsorption of NOM onto P25 ($\rho(TiO_2) = 0.5\ g\ L^{-1}$) over a period of 1 h. No significant change was observed in samples equilibrated for more than 60 min.

for F1, F2 and F3). The preferential adsorption of the larger molecular weight fraction of humic material onto metal oxide surfaces has been reported previously (e.g. [27]). Because the photoinitiated redox reactions leading to the degradation of the NOM occur at or in the immediate vicinity of the TiO_2 surface [28], it follows that F1 will be preferentially degraded as it occupies much more TiO_2 surface compared to both F2 and F3. Moreover, as the adsorbed portion of F1 is degraded, it is to be expected that its place on the TiO_2 surface will be preferentially occupied by F1 from solution rather than by F2 and F3 (either the product of the degradation of F1 or from the original solution). This would lead to F1 being preferentially degraded not only in the initial stages of the reaction, when the pre-adsorbed NOM dominates, but also in later stages, when transport and adsorption from solution supplies the NOM for the ongoing degradation reactions. This is indeed what we observed when the suspensions were irradiated, as shown in Figs. 1 and 2. Thus, differences in the adsorption behavior of the fractions serve to introduce selectivity into an otherwise unselective system.

Comparing these results to those of Brinkmann et al. [18,29] reveals both differences and similarities between the photolytic and the photocatalytic degradation of NOM. A key difference is the velocity of the process, the photocatalytic process being much faster: the changes in the SEC-DOC chromatograms are more extensive after 1 h of irradiation in the presence of TiO_2 than after 24 h in its absence. The steady reduction in DOC content of F1 corresponds well qualitatively to the decrease in the main SEC-DOC peak in samples irradiated in the absence of TiO_2. However, Brinkmann et al. observed a decrease in the height of the main peak with a slight shift of the peak maximum to longer t_r. In contrast, we observe the preferential disappearance of DOC peaks from left to right (shorter to longer t_r) with increasing t_{irrad}. In fact, while the main peak remained the largest after 24 h of irradiation without TiO_2, it clearly wandered to longer t_r before disappearing completely in the presence of TiO_2 within 3 h of irradiation. The peaks constituting F2 and F3 did not change in t_r but only in area. This difference highlights that the main peak assigned to F1 is in fact the result of several overlapping peaks and that these peaks also degraded from left to right as seen in the SEC-DOC chromatograms.

Brinkmann et al. [18,29] also observed the appearance of two additional peaks at longer retention times than the original main peak, and they attributed these additional peaks largely to mono- and dicarboxylic acids. The formation of low molecular weight organic acids in this study is discussed in a later section. Based on the SEC results only, we point out that the relative size of these two "new" peaks is much larger after photocatalysis with TiO_2 than after photolysis. In spite of the difference in degradation pointed out above for F1 and the different relative sizes of the fractions after irradiation, the growth of two smaller fractions at the cost of the larger fraction is common to both processes. The reasons for this, however, are different in each case: while we have given evidence that preferential adsorption of F1 onto the surface of TiO_2 accounts for the observed selectivity in photocatalysis, it is the higher UV absorption of the larger molecules which leads to their faster degradation in photolysis, absorption of photons of sufficient energy being the first step necessary in any photoprocess [30].

The DOC content accessible to analysis by SEC ("chromatographable" dissolved organic carbon, cDOC) is, in general, smaller than the total DOC contained in the sample. This difference is attributed to hydrophobic compounds which remain attached to the column during analysis. The difference between DOC (measured by bypassing the column) and cDOC is then an estimate of the amount of hydrophobic compounds present in the sample. Plotting this difference for the irradiated samples (Fig. 4), we find that hydrophobic compounds are formed in the initial stages of irradiation but are later degraded.

Harmonizing this observation with Fig. 2 is not straightforward because of the many possible underlying processes and the lack of analytical methods suitable for tracing each kind of carbon atom (whether bound in cDOC or not) during the course of irradiation. Since the carbon mass balance is essentially closed for the cDOC (Fig. 2) in the period $0\ min < t_{irrad} \leq 60\ min$, the observed increase in hydrophobic DOC (hDOC) cannot be due to the preferential degradation of hydrophilic constituents or to the formation of hydrophobic coupling products as is often assumed in photolysis [29]. A second possibility is that the hDOC still unaccounted for was initially adsorbed onto the surface of TiO_2 and desorbed upon

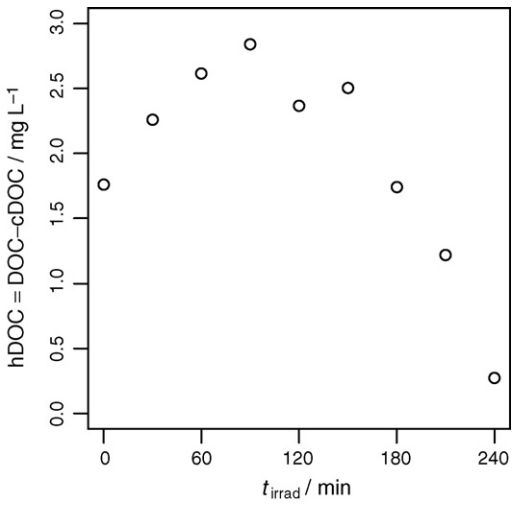

Fig. 4. Formation of hydrophobic compounds during the course of irradiation.

irradiation, thus becoming available for quantification. This desorption could be due to the increased hydrophilic character of the surface induced by the presence of additional charge carriers (electrons and holes) during irradiation—cf. superhydrophilic TiO_2 surfaces [31]. Finally, this result may be due to incomplete mineralization of the DOC during the wet-chemical oxidation prior to detection in our SEC-DOC setup. It is plausible that a part of the hydrophobic compounds in the original Lake Hohloh water only becomes detectable after partial degradation in the irradiated TiO_2 suspensions.

3.2. Size exclusion chromatography with ultraviolet absorbtion detection (SEC-UV)

In the interest of a consistent description, the SEC-UV ($\lambda = 254$ nm) chromatograms were also divided into three fractions, corresponding in retention time to those defined for SEC-DOC as shown in Fig. 5. We point out three differences between the SEC-DOC and SEC-UV chromatograms of the original Lake Hohloh water: first, the appearance of a UV peak with maximum around $t_r = 29$ min, which is very prominent in comparison to its counterpart in the SEC-DOC chromatogram, though small compared to the total area of F1. This prefraction corresponds to totally excluded molecules ($K_D = 0$) with high specific UV absorbance. A second difference is that the main peak in F1 is slightly shifted to shorter t_r compared to the DOC peak. This is an indication that the higher molecular weight material possesses a higher specific UV absorption. And third, F2 and F3 appear smaller in the SEC-UV chromatogram as compared to the SEC-DOC chromatogram. This arises from a lower specific UV absorbance of the lower molecular weight material. These last two observations are in agreement with the results of Uyguner and Bekbölet [9] based on ultrafiltered model humic solutions.

The results from SEC-UV measurements are qualitatively similar to those from SEC-DOC, but the transformations observed upon irradiation occur faster, such that at the end of the irradiation period there is no significant UV absorption of the samples. We sought to quantify the loss of UV absorbing moieties by integrating the SEC-UV chromatograms. These results are shown in Fig. 6. Since NOM contains a variety of UV absorbing groups in unknown quantity and distribution, it is not possible to directly relate UV absorption to each moiety. Therefore, the following is based on overall UV absorption.

Inspection of Figs. 5 and 6 shows a steady decrease in the area corresponding to F1. This was accompanied by a slow increase of both F2 and F3 during the first 60–90 min of irradiation, followed by a slow decrease at longer t_{irrad}. As a consequence, the area under the curve corresponding to F1–F3

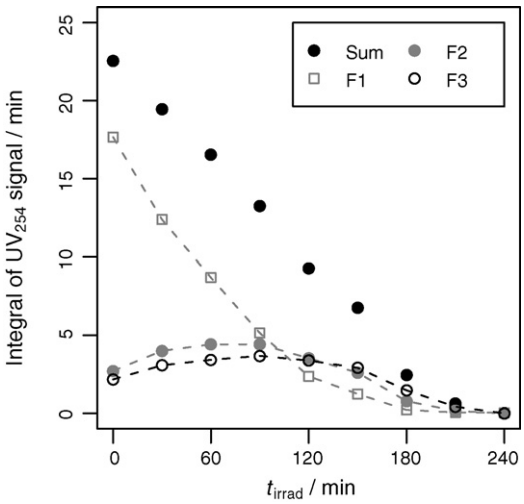

Fig. 6. Integral of the UV_{254} signal for F1–F3 as a function of irradiation time in the presence of $\rho(TiO_2) = 0.5$ g L^{-1}. The dashed lines are intended as a guide to the eye.

decreased steadily with increasing t_{irrad}. This contrasts with the SEC-DOC results where there was no change in the sum of fractions in the first hour of irradiation. This observation is consistent with the expectation that the degradation of larger, UV absorbing molecules leads to the formation of less UV absorbing metabolites through the loss of double bonds, which are nonetheless still part of the DOC.

While we observed the overall disappearance of UV absorbing groups when considering F1, F2 and F3 together, F2 and F3 initially experienced an increase in UV absorption. We attribute the increase in F2 to UV absorbing metabolites of F1 that become part of F2 because of reduced molecular size. Similarly, we attribute the increase in UV absorption of F3 to metabolites of both F1 and F2. This contrasts with the results of Brinkmann et al. [18,29], who did not observe UV absorption corresponding to the peaks we have assigned to F2 and F3. These two differences, the "sequential" disappearance of F1 from shorter to longer t_r and the UV absorption of F2 and F3, indicate that the photolytic and photocatalytic processes not only proceed at different velocities but also lead to different products and size distributions of the metabolites of the original NOM.

Comparing the results in Fig. 5 with results from the reaction of •OH (generated through the UV/H_2O_2 process, homogeneous) with NOM [32] shows both similarities and differences. Similar is the steady breakdown of larger UV absorbing molecules to form smaller molecules, some of which retain UV absorbing

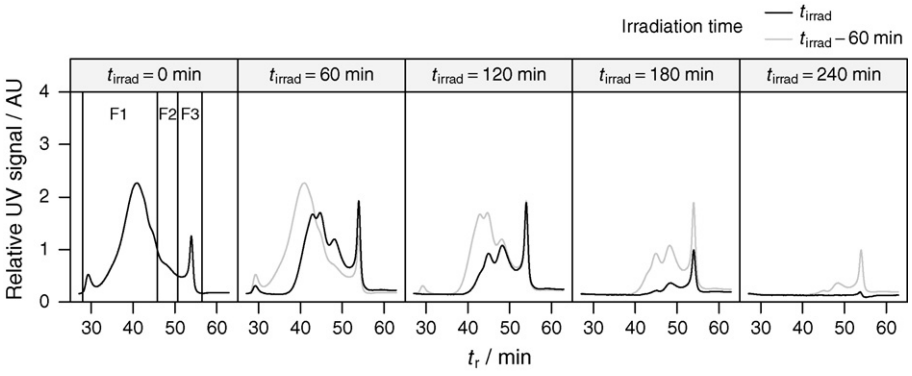

Fig. 5. SEC-UV chromatograms showing the time evolution of F1–F3 under UV irradiation in the presence of $\rho(TiO_2) = 0.5$ g L^{-1}.

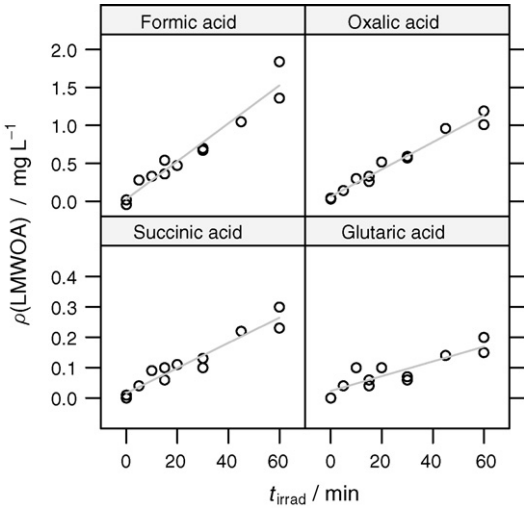

Fig. 7. Formation of low molecular weight organic acids.

properties. Different is the progression of the degradation: whereas the peak in F1 is seen to both be reduced in size and to wander towards longer t_r in Fig. 5, the corresponding peak in the case of UV/H_2O_2 is also reduced in size but its onset does not wander to longer t_r. We attribute this difference to differences in the localization of the reaction: in the case of the TiO_2 suspensions, the reaction occurs near the surface of the particles; thus, adsorption of NOM to the surface of TiO_2 is important as discussed in Section 3.1. In the case of the UV/H_2O_2 process, the reaction of •OH with NOM occurs throughout the volume of the solution and the •OH have equal access to all NOM size fractions proportional to their concentration. A comparison on the basis of DOC results is not possible because Sarathy and Mohseni [32] only report SEC-UV data.

3.3. Formation of low molecular weight organic acids (LMWOA)

The formation of four small organic acids, namely formic, oxalic, succinic and glutaric acids was followed by means of ion chromatography. In addition to these acids, acetic and malonic acids were identified as being produced but could not be quantified due to interfering peaks and poor reproducibility in the chromatograms. Injection of the single compounds in the SEC system showed that all three dicarboxylic acids elute primarily in F2 while formic acid elutes with F3.

In irradiation experiments with $t_{irrad} \leq 60$ min, the concentration of all four LMWOA increased linearly with t_{irrad} (Fig. 7). The amounts of acid produced followed the order formic > oxalic ≫ succinic > glutaric. Formic acid accounted for roughly 10% of the DOC in F3 after 30 and 60 min of irradiation, with increasing tendency. The sum of the dicarboxylic acids (oxalic, succinic, glutaric) accounted for a similar proportion of the DOC in F2.

Longer irradiation experiments ($t_{irrad} \leq 240$ min) revealed that the concentration of oxalic acid plateaus between the measurements at $t_{irrad} = 90$ min and $t_{irrad} = 120$ min with a value of ≈ 1.5 mg L^{-1} ($\approx 10\%$ of the DOC in F2) and later decreases monotonically. The concentration of formic acid showed a maximum value after $t_{irrad} = 150$ min (≈ 3.2 mg L^{-1}, $\approx 20\%$ of the DOC in F3). The maxima observed in the concentration of formic and oxalic acids correlate well with the maxima in DOC (shown in Fig. 2).

3.4. Bioavailability of the DOC

To assess the bioavailability of the DOC before and after irradiation in the presence of TiO_2, samples (0 min < t_{irrad} < 60 min) were incubated with an activated sludge inoculum for 2 days and then examined by means of SEC-DOC. These chromatograms are shown in Fig. 8. Addition of the inoculum was observed to bring in a significant amount of DOC, the largest part of which eluted with $K_D > 1$. These additional DOC peaks were, however, no longer present after the incubation period.

The non-irradiated sample showed little or no change in DOC content of the peaks corresponding to F2 and F3 ($|\Delta DOC_{F2}| < 0.5$ mg L^{-1}, $|\Delta DOC_{F3}| < 0.1$ mg L^{-1}). However, the range corresponding to F1 showed both an increase (peak with maximum around $t_r = 30$ min) and a decrease (starting at about $t_r = 34$ min) in DOC, for an overall loss of ≈ 0.75 mg L^{-1} DOC. This was unexpected, as previous biodegradation studies had shown essentially no degradation of the region assigned here to F1 upon bacterial incubation [18]. A possible reason for this are the different bacterial cultures used: whereas the inoculum used in [18] was obtained from the Lake Hohloh water itself, the inoculum used in this study contained activated sludge from two different wastewater treatment plants (one industrial, one municipal). It is attractive to assume that the inoculum from activated sludge contained a larger microbial diversity with a correspondingly larger metabolic potential than the inoculum from Lake Hohloh.

With increasing irradiation time, the net DOC decrease in F1 became smaller, while the net positive part of the difference

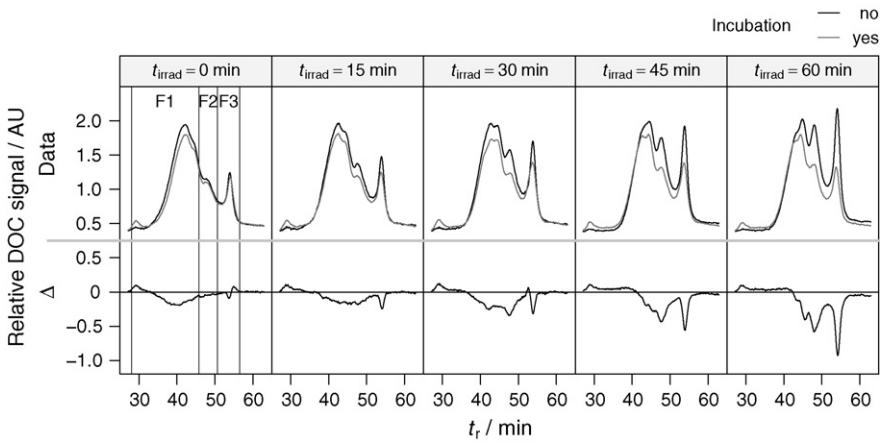

Fig. 8. SEC-DOC chromatograms of irradiated samples (0 min < t_{irrad} < 60 min) before and after incubation with a mixed bacterial culture for 2 days.

spectrum appeared to extend to longer retention times. This points to a synthesis of higher molecular weight organic substances by the bacteria. Integrating only the net positive part of the difference spectra (bottom spectra in Fig. 8) reveals an increasing trend in area which is nevertheless $< 0.1\ mg\ L^{-1}$.

The amount of bioavailable DOC contained in F2 increased from $\approx 0.4\ mg\ L^{-1}$ for the non-irradiated sample to $\approx 1.6\ mg\ L^{-1}$ after 60 min of irradiation. At the same time, the bioavailable DOC in F3 steadily increased from approximately 0 to $\approx 1.7\ mg\ L^{-1}$ at $t_{irrad} = 60$ min. Taking into consideration that formic acid elutes mostly with F3 and all other acids elute largely in F2, the quantified LMWOA account for 25–30% of the bioavailable DOC in F2 and $\approx 20\%$ in the case of F3. Thus, these acids, along with malonic and acetic acids which were detected but could not be quantified, form an important part of the bioavailable DOC.

It is interesting to note that the chromatograms after incubation changed only minimally for the range of t_r corresponding to F2 and F3, while the range corresponding to F1 changed extensively. This further supports the notion of a sequential photocatalytic degradation of the DOC fractions in order of decreasing molecular size. Furthermore, it shows that a large fraction of the metabolites present after irradiation are bioavailable.

4. Conclusions

The photocatalytic degradation of humic-rich natural organic matter from a bog lake was found to proceeded in a sequential manner, starting from the larger molecular size fraction and proceeding towards smaller molecular size fractions and giving rise to the production of bioavailable products, including small molecular weight organic acids. As a result, no significant mineralization was observed in the initial stage of the reaction, followed by steady mineralization after this lag phase. This correlated well with the preferential adsorption of the larger molecular weight fraction of the NOM onto the surface of the TiO_2 photocatalyst, which favors its degradation.

Comparison of these results with the degradation of NOM through UV irradiation alone and through the homogeneous reaction of $^{\bullet}OH$ with NOM points to different molecular size distribution and chemical structure of the metabolites. This can have implications on the potential for byproduct formation during and for bacterial regrowth after water treatment.

Acknowledgements

This work was funded in part by the German Technical and Scientific Association for Gas and Water (DVGW). We are grateful to Elly Karle, Rafael Peschke, and Lena Reichert for the measurement of the small organic acids.

References

[1] F.H. Frimmel, G. Abbt-Braun, K.G. Heumann, B. Hock, H.-D. Lüdemann, M. Spiteller (Eds.), Refractory Organic Substances (ROS) in the Environment, Wiley, New York, 2002.
[2] C. Zwiener, T. Reemtsma, M. Jekel (Eds.), Organic Pollutants in the Water Cycle, Wiley-VCH, Weinheim, 2006, pp. 251–286.
[3] O. Legrini, E. Oliveros, A.M. Braun, Chem. Rev. 93 (1993) 671–698.
[4] T. Oppenländer, Photochemical Purification of Water and Air, Wiley-VCH, Weinheim, 2003.
[5] S. Malato, J. Blanco, D.C. Alarcón, M.I. Maldonado, P. Fernández-Ibáñez, W. Gernjak, Catal. Today 122 (2007) 137–149.
[6] S. Ogawa, M. Tanigawa, M. Fujioka, Y. Hanasaki, Jpn. J. Toxicol. Environ. Health 41 (1995) 7.
[7] M. Bekbölet, Z. Boyacioglu, Özkaraova, Water Sci. Technol. 38 (1998) 155–162.
[8] M. Bekbölet, A.S. Süphandağ, C.S. Uyguner, J. Photochem. Photobiol. A 148 (2002) 121–128.
[9] C.S. Uyguner, M. Bekbölet, Catal. Today 101 (2005) 267–274.
[10] X.Z. Li, C.M. Fan, Y.P. Sun, Chemosphere 48 (2002) 453–460.
[11] F.L. Palmer, B.R. Eggins, H.M. Coleman, J. Photochem. Photobiol. A 148 (2002) 137–143.
[12] R. Al-Rasheed, D.J. Cardin, Appl. Catal. A 246 (2003) 39–48.
[13] J. Wiszniowski, D. Robert, J. Surmacz-Gorska, K. Miksch, J.-V. Weber, Int. J. Photoenergy 5 (2003) 69–74.
[14] C.S. Uyguner, M. Bekbölet, Int. J. Photoenergy 6 (2004) 73–80.
[15] A. Kerc, M. Bekbölet, A.M. Saatci, Water Sci. Technol. 49 (2004) 7–12.
[16] J. Wiszniowski, D. Robert, J. Surmacz-Gorska, K. Miksch, J.V. Weber, J. Photochem. Photobiol. A 152 (2002) 267–273.
[17] G. Hua, D.A. Reckhow, Environ. Sci. Technol. 41 (2007) 3309–3315.
[18] T. Brinkmann, P. Hörsch, D. Sartorius, F. Frimmel, Environ. Sci. Technol. 37 (2003) 4190–4198.
[19] T.E. Doll, F.H. Frimmel, Chemosphere 52 (2003) 1757–1769.
[20] A. Defoin, R. Defoin-Straatmann, K. Hildenbrand, E. Bittersmann, D. Kreft, H.J. Kuhn, J. Photochem. 33 (1986) 237–255.
[21] S.A. Huber, F.H. Frimmel, Anal. Chem. 63 (1991) 2122–2130.
[22] C.H. Specht, F.H. Frimmel, Environ. Sci. Technol. 34 (2000) 2361–2366.
[23] S.A. Huber, A. Balz, F.H. Frimmel, Fresen. J. Anal. Chem. 350 (1994) 496–503.
[24] F.H. Frimmel, J. Contam. Hydrol. 35 (1998) 201–216.
[25] P. Westerhoff, G. Aiken, G. Amy, J. Debroux, Water Res. 33 (1999) 2265–2276.
[26] A.W.P. Vermeer, W.H. van Riemsdijk, L.K. Koopal, Langmuir 14 (1998) 2810–2819.
[27] A.W.P. Vermeer, L.K. Koopal, Langmuir 14 (1998) 4210–4216.
[28] A.L. Linsebigler, G. Lu, J.T. Yates, Chem. Rev. 95 (1995) 735–758.
[29] T. Brinkmann, D. Sartorius, F.H. Frimmel, Aquat. Sci. 65 (2003) 415–424.
[30] A.M. Braun, M.-T. Maurette, E. Oliveros, Photochemical technology, Wiley, Chichester, 1991.
[31] A. Fujishima, K. Hashimoto, T. Watanabe, TiO_2 Photocatalysis—Fundamentals and Applications, Bkc, Inc., Tokyo, 1999.
[32] S.R. Sarathy, M. Mohseni, Environ. Sci. Technol. 41 (2007) 8315–8320.